



Hydrogeophysical investigation of aquifer parameters and seawater intrusion: a case study from Eastern Mitidja plain, Algeria

Z. Nemer · F. Khaldouï · Z. Benaïssa ·
A. Belaroui · M. Y. Tebbouche · A. Ydri

Received: 25 January 2022 / Accepted: 9 May 2023
© The Author(s) 2023

Abstract The rapid depletion of surface water due to climate change increases the world's water demand. As a result, groundwater resources are rapidly emerging as the primary source of freshwater supply for various needs. However, overexploitation and inadequate management of these resources can lead to irreversible contamination of freshwater reservoirs. Effective groundwater resource management depends on a detailed understanding of hydrogeological parameters that control the complex functioning of aquifers. However, these data are often scarce due to their expensive acquisition process. The present study assesses the use of geophysical methods for the estimation of hydrogeological parameters namely hydraulic conductivity and transmissivity. Moreover, the study evaluates the marine intrusion in the coastal aquifer of one of the most important plains of

Algeria. The approach suggested is based on a combination of cost-effective geophysical techniques (geo-electrical surveys) and precise hydrogeological data. The results identified aquifer parameters relevant to the location of new water wells and allowed delineation of the seawater/freshwater interface.

Highlights

- Groundwater resources are rapidly emerging as the primary source of freshwater supply due to the rapid depletion of surface water caused by climate change.
- Effective groundwater resource management requires a detailed understanding of hydrogeological parameters that control the complex functioning of aquifers, but acquiring this data can be expensive and difficult.
- The study assesses the use of cost-effective geophysical techniques (geo-electrical surveys) for estimating hydrogeological parameters, specifically hydraulic conductivity and transmissivity.
- The study also evaluates marine intrusion in the coastal aquifer of one of the most important plains of Algeria, and the results allowed for the identification of relevant aquifer parameters for the location of new water wells and the delineation of the seawater/freshwater interface.

Z. Nemer (✉) · F. Khaldouï · Z. Benaïssa · A. Ydri
Geophysics Laboratory, Faculty of Earth Sciences
Geography and Territorial Planning (FSTGAT), University
of Sciences and Technology Houari Boumediene
(USTHB), Algiers, Algeria
e-mail: znemer@usthb.dz

A. Belaroui
Geo-Environment Laboratory, Faculty of Earth Sciences
Geography and Territorial Planning (FSTGAT), University
of Sciences and Technology Houari Boumediene
(USTHB), Algiers, Algeria

M. Y. Tebbouche
Institute of Architecture and Earth Sciences (IAST),
University Ferhat Abbas Sétif 1 (UFAS), Sétif, Algeria

Keywords Hydrogeophysics · Aquifer parameters · VES · Groundwater · Eastern Mitidja Plain · Transmissivity · Hydraulic conductivity

1 Introduction

The demand for water is significantly increasing worldwide due to rapid population growth, industrial development, and climate change. Furthermore, by 2050, industrial demand for water is expected to put tremendous pressure on the accessibility of freshwater, reducing the amount of clean water for agriculture and domestic uses (Islam and Karim 2019). The depletion and pollution of surface water (dams, lakes) prompted many countries to explore groundwater resources. Currently, groundwater is the world's most extracted resource, with withdrawal rates estimated at 982 km³/year (Margat and Gun 2013). Approximately 70% of the extracted volumes are used for agriculture and supplies half of the world's demand for drinking water (Cross et al. 2016).

Aquifers occur in different geological formations at varying depths. An understanding of these formations' hydrodynamics is fundamental to access and exploit the resource. However, the required parameters are collected using extremely expensive and time consuming pumping tests that provide only point-in-time information (Bateni et al. 2015). The major parameters used to describe groundwater potential include Transmissivity (T), expressed as the rate at which groundwater can flow through an aquifer section of unit width under a unit hydraulic gradient, and Hydraulic Conductivity (K), defined as the ease with which water can move through an aquifer. On the other hand, geophysical techniques have been extensively used in hydrogeological studies. Indeed, geoelectrical methods proved to be highly effective in groundwater exploration considering the strong correlation between the resistivity and the formation properties (water content, fluid composition, permeability) (Park et al. 2016). This relationship provides interesting insights into aquifer conditions, including water table depth, saturated thickness, and water salinity. These non-destructive geoelectrical methods have been successfully applied in various applications including: groundwater exploration (Benabdellouahab et al. 2019), delineation of landfills and solute transfers (Mepaiyeda et al. 2019), agricultural management

by identifying areas of excessive compaction or thickness of soil horizons and bedrock depth (Samouëlian et al. 2005), and determination of soil hydrological properties (Pozdnyakova et al. 2001). Moreover, recently, geoelectrical data has emerged as a powerful tool to estimate the above-mentioned hydrogeological parameters (T and K) (Akhter et al. 2022; El Osta et al. 2021; Hasan et al. 2021; Kenneth and Ebifuro 2012; Tijani et al. 2021).

This method produces geoelectrical columns and cross sections that describe vertical and lateral variations in soil properties (Binley 2015). These results require few pumping tests and lithological logs to properly correlate resistivity and hydrogeological properties (Hasan et al. 2020b). Alternatively, a combination of the various derived properties (thicknesses and resistivity) could be used to produce additional information to accurately characterize the study area. These are referred to as Dar Zarrouk parameters (transverse resistance and longitudinal conductance). They are widely used in groundwater assessment and can help overcome the "non-unique solution" of electrical resistivity interpretation (Niwas and Singhal 1981; Utom et al. 2012). Furthermore, these parameters are linked to the groundwater salinity, which helps to assess water quality over large areas (Ebang et al. 2014).

As many countries of the world, Algeria is experiencing significant population growth, particularly in its northern part, the center of its economic activities¹. This growth, combined with industrial development and climate variability, exerts significant stress on water resources. Moreover, groundwater is the main source of fresh water for drinking, irrigation and industrial needs in Algeria. As the demand for water increases, Algerian authorities approve the construction of new water wells. However, an increase in the number of wells can lead to serious sustainability and environmental threats for the resource, such as depletion and pollution, particularly if the wells are randomly implanted (Konikow and Kendy 2005). Indeed, the location and number of wells must be carefully considered to ensure sustainable groundwater management. The placement of wells is based on aquifer parameters and properties, which are usually non-existent or scarce. To this end, vertical electrical sounding, a geophysical method, is used to assess groundwater potential, determine aquifer properties, and assist authorities in identifying appropriate areas

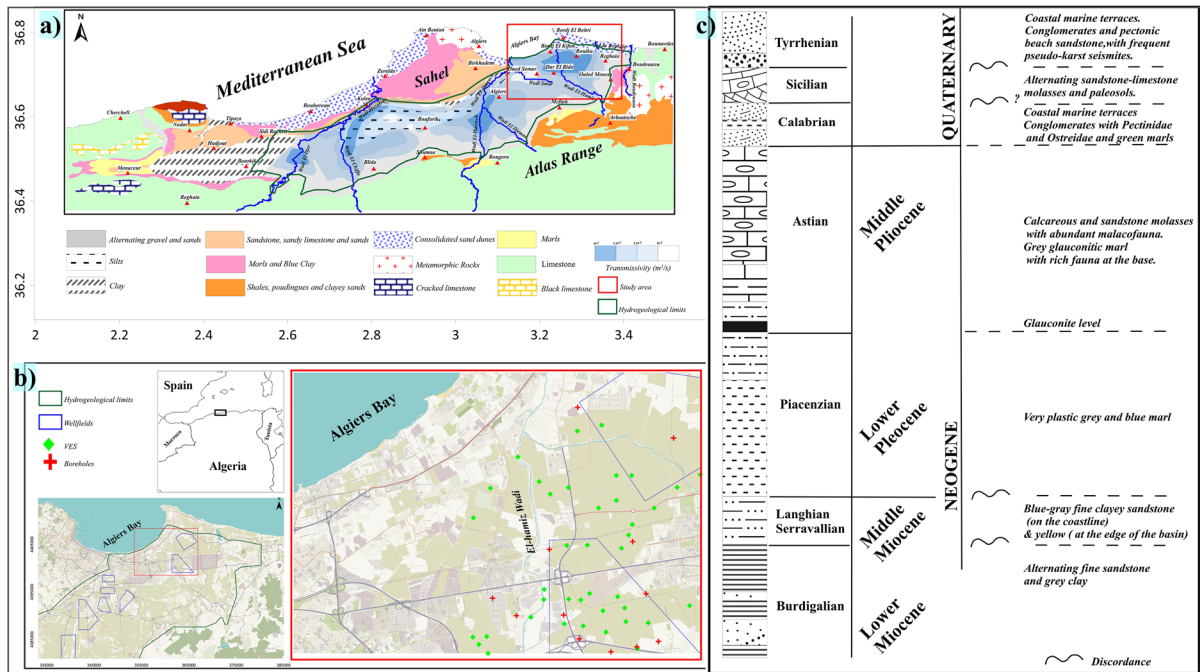


Fig. 1 Study area presentation. **a** Geological map of the Mitidja plain. **b** Location of the study area. **c** Schematic stratigraphic log of the Neogene and Quaternary based on the work

of Glangeaud et al. (1952), Aymé (1952), Betrouni (1983), Djediat (1996, 2013), Yassini (1973)

for well locations while ensuring the resources sustainability (Kosinski and Kelly 1981).

Furthermore, coastal aquifers are often at risk of seawater intrusion, a serious threat to the sustainability of this resource worldwide (Moore and Joye 2021). This irreversible phenomenon is described as the lateral and vertical migration of saltwater due to intensive groundwater withdrawal, resulting in severe degradation of groundwater quality². Monitoring saltwater intrusion is crucial when implanting water wells and setting up their pumping rates. The present study is conducted in the eastern part of the Mitidja plain, one of the largest and most fertile coastal plains in Algeria. This site was chosen because of its agricultural and socio-economic importance. Indeed, the groundwater resources in this region supply the entire city of Algiers and its surroundings. Nevertheless, a number of potential concerns have been reported in this area, such as seawater intrusion (Belaidi and Salhi 2010), nitrate pollution (Hadjoudj et al. 2014) and groundwater depletion (ANRH 2012). The aim of this case study is, first, to evaluate the applicability of geoelectrical methods to estimate different hydraulic

parameters and, second, to assess marine intrusion in Algiers Bay and address the potential implementation of new wells in this area.

2 Study area

The Mitidja plain emerged following the post-Miocene tectonic activity. It is located between two positive units: the Atlas Range to the south that continues to elevate until today and the Sahel to the north that separates the plain from the Mediterranean Sea (Fig. 1a). The alluvial plain of the Mitidja formed after a post-Miocene subsidence with a NE-SW main axis between longitudes 2° 19' E and 3° 33' E, and latitudes 36° 24' N and 36° 49' N. The plain extends over 100 km from east to west and 3 to 18 km from north to south with an average altitude of 100 m. It is limited to the north by the Sahel of Algiers (260 m altitude), to the south by the Bidean Atlas (1630 m altitude), to the west by Mount Bou Mad (1560 m altitude), and to the east by the sand dunes of Ain Taya and the Mediterranean Sea. The basin is covered

by Pliocene to Quaternary sediments overlying a resistant bedrock (Fig. 1c).

Two main aquifers were formed as a result of the geological and geomorphological development of the Mitidja during the Pliocene and Quaternary:

- a. *The Astian reservoir*: It is delimited between a Plaisancian clay substratum and a thick marly cover and mainly composed of sandstone or calcareous sandstone. However, its distribution is not well defined and only its outcrops in the Sahel are known. It is limited to the north by the southern edge of the Sahel and it disappears upstream, towards the south, along a SW-NE line running through Boufarik and El-Affroun. This reservoir's depth varies between 200 and 400 m with an average thickness estimated at 100 m. It is recharged mainly by rainfall infiltration on the Sahel and in the Atlas piedmonts. The only outlets of this aquifer are some privileged vertical percolations towards the quaternary aquifer through thin layers of yellow marls or gravelly deposits.
- b. *The Quaternary aquifer*: it is essentially formed by the superposition of the middle Quaternary alluvium and the lower part of recent alluvium. The basement of this reservoir is the top of the marly cover that presents a shoals morphology separated by deeply incised pockets and channels, in which the permeable sediments reach a thickness of 80–100 m. These alluvial masses are isolated from each other by the non-eroded yellow marls that are sub-cropping and define sterile zones. This aquifer is recharged by rainfall infiltration in the plain (60%), infiltration of rivers in the Atlas piedmonts (30%), seepage through the borders of the sahel (7%) and drainage from the Astian to the alluvial aquifer, through variable marl thickness (3%). The latter case is not well studied and established since areas where aquifers are in contact are not clearly identified.

The quaternary aquifer is the most promising but is not homogeneous. Indeed, it is characterized by an uneven distribution of sandy gravels. On the horizontal, pockets and channels with good transmissivity alternate with layers of poor transmissivity. On the vertical, the alluvial deposits are heterogeneous due to morphoclimatic factors. On the other hand, the

exploitation of the Astian aquifer is not particularly interesting since, deprived of an outlet; it restores its limited resources to the alluvial aquifer. From a hydrodynamic perspective, the transmissivity is low on the marl deposits and the Atlas piedmonts: 1 to 5×10^{-3} m²/s, but reaches 40×10^{-3} m²/s in the Chiffa, Bas Mazafran, El-Harrach channels and in the Rouïba alluvial pocket. The high variability of transmissivity may be due to abrupt changes in layers thickness. The permeability is relatively constant: 1 to 1.5×10^{-3} m²/s and the storage coefficient ranges between 3 and 10% (ANRH 1977).

3 Data and methods

3.1 Data acquisition

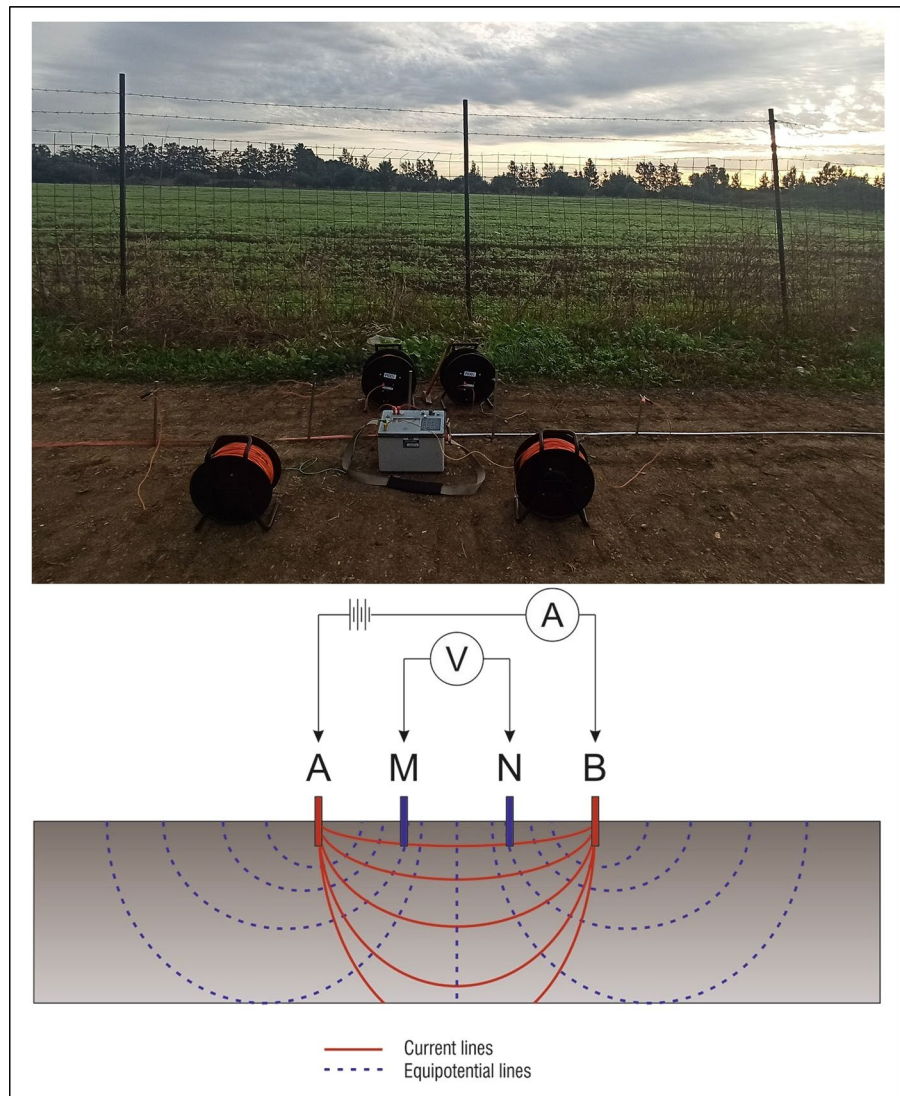
Geoelectrical methods are particularly interesting in hydrogeology as they can help distinguish freshwater from saltwater (Hasan et al. 2018), soft rock sand aquifers from clay materials (Mlangi et al. 2018), porous/fractured hard rock aquifers of low permeability clays and marls (Singhal and Gupta 1999), and fractured rock aquifers of their solid host rock (Adepelumi et al. 2006).

The principle of surface electrical resistivity surveys is based on the premise that the electrical potential distribution in the ground surrounding a current-carrying electrode depends on the electrical resistivity and distribution of the underlying soils and rocks. Typical field design involves applying a direct electrical current (DC) between two soil-implanted electrodes and then measuring the potential difference between two additional electrodes. The potential electrodes are commonly placed between the current electrodes, but they can be located anywhere in the field. The data from resistivity surveys are usually reported as apparent resistivity values ρ_a (Ginzburg 1974) given as the resistivity of an electrically homogeneous and isotropic half-space that would give the measured relationship between the applied current (I) and the potential difference (U) for a particular arrangement and spacing of the electrodes as follows:

$$\rho_a = k \cdot \frac{U}{I} \quad (1)$$

where ρ_a is the apparent resistivity in (Ω m), K is the geometric factor in (m) calculated as follows:

Fig. 2 Schematic configuration of VES acquisition array



$$k = \frac{1}{2\pi} \left\{ \left(\frac{1}{AM} - \frac{1}{BM} \right) - \left(\frac{1}{AN} - \frac{1}{BN} \right) \right\},$$

U is the potential in (V), I is the current in (A).

Apparent resistivity is measured at a single location or around a central point by systematically varying electrode spacing. This procedure is often referred to as vertical electrical sounding (VES), or vertical profiling. A VES survey is ideally designed to determine the number, thickness, and resistivity of layers (Kneisel and Hauck 2008). The basic vertical resistivity profiling approach is to gradually increase the spacing of AB current injection electrodes, leading to deeper penetration of the current line and, therefore, increased influence of deeper layers on

apparent resistivity. These are plotted versus current electrode spacing on a log/log scale and interpolated into a continuous curve. This is called the sounding curve and serves as a prerequisite for any data inversion required to derive the resistivity/depth structure of the soil. The most common configurations in a 1D resistivity survey are Schlumberger, Wenner, and Dipole–Dipole. For practical and methodical reasons, vertical electrical surveys most often use the symmetrical Schlumberger configuration, in which the voltage electrodes M, N are close and fixed in the center of the array and the current electrodes A, B move outward (Fig. 2). A detailed discussion of the theoretical

background can be found in (Mundry and Dennert 1980).

After the data collection, an inversion process is necessary to determine the number of layers, their resistivity and their thickness. Unlike the theoretical approach, this is not a simple matter in the context of data distribution. The inversion is based on comparing measured sounding curves with calculated sounding curves for a given layer model (Haldar 2013). Initially, formalized master curves and graphical procedures were used (Narayan et al. 1994). Today, computer programs are widely available that allow rapid computation for any number of layers. Some of these programs are fully automated without any layering assumptions, while others requires the intervention of an interpreter (Massoud et al. 2015). In the latter case, a base model is created by incorporating existing geological parameters (e.g., thickness of stratigraphic units, depth to water table), available drilling data, or additional geophysical data (Mantovani 2016). The computer program attempts to fit both the theoretical model and borehole data to the measured curve through an iterative process. The "best fit" to stop the iteration can be defined by the computer using a root mean square (RMS) error or preferably by the interpreter (Zohdy et al. 1974).

Subsurface resistivity is mainly controlled by the pore arrangement, the amount of pore water and its resistivity. Therefore, in coarse-grained soils, the groundwater interface is usually marked by an abrupt change in water saturation and consequently a change in resistivity. Whereas, in fine-grained soils, such a change in resistivity may not occur concurrently with a water table surface. Therefore, a wide range of resistivity for any particular soil or rock type exists. In addition, resistivity values cannot be directly interpreted in terms of soil type or lithology. However, distinct resistivity values can be associated with specific rock units based on local geology or borehole information.

Geoelectrical techniques have some inherent limitations that alter its resolution and accuracy. Similar to any method that involves the measurement of a potential field, a measurement value obtained at a given location represents a weighted average of the effects produced over a large volume of material, with the nearest parts contributing the most. This tends to produce smooth curves, not suitable for high

resolution interpretations. A further characteristic common to all potential field geophysical methods is that a particular potential distribution at the ground surface does not generally have a unique interpretation. Although these limitations must be recognized, the non-uniqueness or ambiguity of the resistivity method is only slightly less than for other geophysical methods (Abdelrahman et al. 2008).

In this study, 40 VES were conducted throughout the study area using a schlumberger array with a maximum half-current electrode spacing of 350 m (AB/2) (Fig. 1b). The collected data were processed using IP2WIN software. The threshold for the RMS error was set at 5%. Supplementary geological and hydrogeological data from nine boreholes available in the study area were used to calibrate the geophysical data and validate the results.

3.2 Dar-Zarrouk parameters

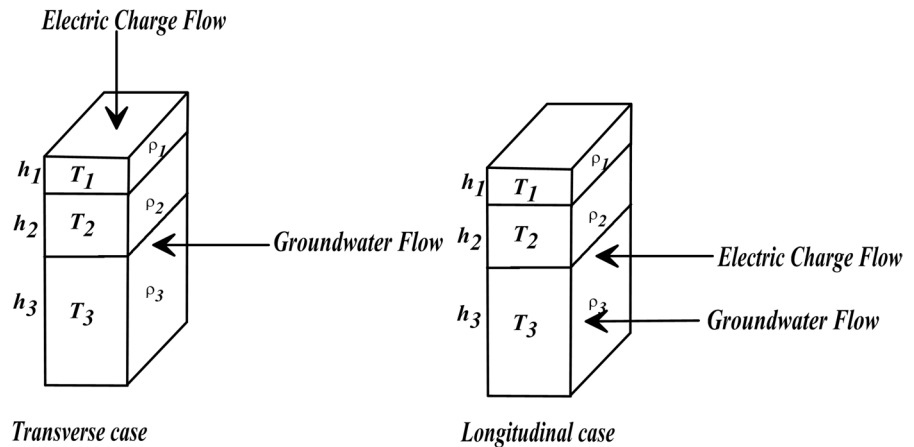
Dar-Zarrouk parameters were first introduced by Maillet (1947). For n horizontal, homogeneous and isotropic layers of resistivity ρ_i and thickness h_i (Fig. 3), the longitudinal unit conductance \mathbf{S} and the transverse unit resistance \mathbf{T}_r are defined as:

$$T_r = \sum_{i=1}^n h_i * \rho_i (\Omega m^2) \quad (2)$$

$$S = \sum_{i=1}^n \frac{h_i}{\rho_i} (\text{mhos}) \quad (3)$$

These two parameters and the concept derived from Dar-Zarrouk curves are essential in the development of the interpretation theory for vertical electrical soundings (Singh et al. 2003). For particular applications in groundwater studies, \mathbf{S} and \mathbf{T}_r emerge as powerful independent interpretation tools apart from any comprehensive interpretation scheme. Their application extend beyond the usual hydrogeological applications of resistivity soundings usually focused on defining the aquifer geometry. Indeed, the combination of thickness and resistivity into a single variable is used to assess many properties including aquifer transmissivity, storage, and protective capacity (Henriet 1976).

Fig. 3 The theory and application of D-Z parameter in a geoelectrical column



3.3 Electrical anisotropy

Electrical anisotropy refers to a pattern in which rock resistivity is generally lower parallel to the bedding than transversal to the bedding (Bahr 2007). In vertical electrical soundings, the current flow lines are curved, therefore transverse resistivity ρ_t and longitudinal resistivity ρ_l are encountered along with an anisotropic coefficient λ . They are expressed as follows:

$$\rho_l = \frac{\sum h_i}{S} (\Omega m) \tag{4}$$

$$\rho_t = \frac{T_r}{\sum h_i} (\Omega m) \tag{5}$$

$$\lambda = \sqrt{\frac{\rho_t}{\rho_l}} \tag{6}$$

3.4 Estimation of transmissivity and hydraulic conductivity

Hydraulic parameters \mathbf{T} and \mathbf{K} are important for estimating groundwater reserves. However, these are acquired by expensive and time-consuming pumping tests. Consequently, a simple and easy approach capable of accurately estimating these parameters is needed. Lately, the combination of pumping tests and geoelectrical data has proven to be effective in such cases (El Osta et al. 2021; Hasan et al. 2017). In this study, the Kozeny–Carman–Bear formula (Bear and

Braester 1972) was used to estimate the hydraulic conductivity (\mathbf{K}) using the following formula:

$$K = \frac{\delta_w * g}{\mu} * \frac{d^2}{180} * \frac{\varphi^3}{(1 - \varphi)^2} \tag{7}$$

where \mathbf{K} : hydraulic conductivity (m/day); φ : porosity; d : grain size; g : gravity acceleration (9.81 m/s^2); μ : dynamic viscosity of water (0.0014 kg/ms); δ_w : density of the fluid (1000 kg/m^3).

The porosity is obtained from the Archie equation as follows:

$$\rho_a = \alpha \rho_w \varphi^{-m} \tag{8}$$

From (8):

$$\varphi = e^{\left(\frac{1}{m}\right) \ln \alpha + \left(\frac{1}{m}\right) \ln \left(\frac{1}{F_i}\right)} \tag{9}$$

with

$$F_i = \frac{\rho_o}{\rho_w} \tag{10}$$

and

$$\rho_w = \frac{10000}{EC} \tag{11}$$

ρ_o : The bulk resistivity, ρ_a : aquifer resistivity from the VES data, φ : porosity of aquifer medium, F_i : intrinsic formation factor valid for clay free formation, α : coefficient of saturation, m : cementation factor, ρ_w : groundwater resistivity, EC : electrical conductivity ($\mu\text{S/cm}$).

The values of m and α required in Eq. (9) are essential to calculate porosity. They must be

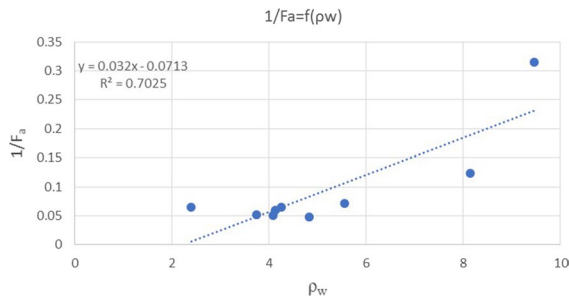


Fig. 4 Curve of $1/F_a$ versus water resistivity ρ_w

determined at each study site through laboratory tests. However, due to the lack of core samples within the study area, an alternative approach was used, in which a wide range of α and m values reported in the literature were taken to derive porosity estimates. Indeed, Worthington (1993) reported three different expressions for the intrinsic formation factor in relation to the porosity of samples from different locations. Moreover, Jackson et al. (1978) and de Lima and Sharma (1990) suggested another expression in which the coefficient α is equal to 1 while m varies from 1.3 to 2.5. For this study, $\alpha = 1$ and m ranging from 1.49 to 1.97 were used in Eq. (9) to calculate porosity.

However, Eq. (9) is only valid for clay-free media. For a clay rich aquifer, an iteration of Archie's equation is required. The survey area contains a significant amount of clay. Therefore, we use the following Waxman-Smits model (Waxman and Smits 1968) for the clay medium:

$$F_a = F_i(1 + BQ_v\rho_w)^{-1} \quad (12)$$

BQ_v : depend on surface conduction effects. If surface conduction is non-existent, then F_a becomes equal to F_i .

$$\frac{1}{F_a} = \frac{1}{F_i} + \frac{BQ_v}{F_i}\rho_w \quad (13)$$

In the above equation, $1/F_a = \rho_w/\rho_o$. A linear relationship between $1/F_a$ and ρ_w is depicted in Eq. 13. In this case, BQ_v/F_i represents the slope, and $1/F_i$ indicates the intercept for the straight

line. Consequently, the intrinsic formation factor was obtained from the curve relating $1/F_a$ and ρ_w (Fig. 4) to calculate the porosity using Eq. (9). Subsequently, K values were determined for all nine VES points conducted near boreholes.

Consequently, transmissivity (T) was determined for the same selected nine VES locations. T is given as:

$$T = K * h \quad (14)$$

K : hydraulic conductivity (m^2/d), h : aquifer thickness (m).

From Eq. (5):

$$Tr = \rho * h \quad (15)$$

Thus, from Eqs. (14) and (15)

$$T = \frac{Tr * K}{\rho} \quad (16)$$

$$K = \frac{\rho * T}{Tr} \quad (17)$$

From Eqs. (16) and (17)

$$T \leftrightarrow T_r$$

$$K \leftrightarrow \rho_a$$

The above Eqs. (16) and (17) show a direct relation between T and T_r , and K and respectively. In order to estimate transmissivity (T) and hydraulic conductivity (K) for all sounding stations, the following relations were obtained from the plots of T versus T_r and K versus ρ_a for the selected sounding stations near 9 wells as shown in Fig. 5:

$$T = 0.125(T_r) + 108 \quad (18)$$

$$K = 0.0901(\rho_a) + 3.28 \quad (19)$$

All calculated parameters for the nine VES locations are listed in Table 1. These were compared to values obtained from the pumping tests for validation. Then, values of K and T at locations where pumping tests were not available were estimated using Eqs. 18 and 19.

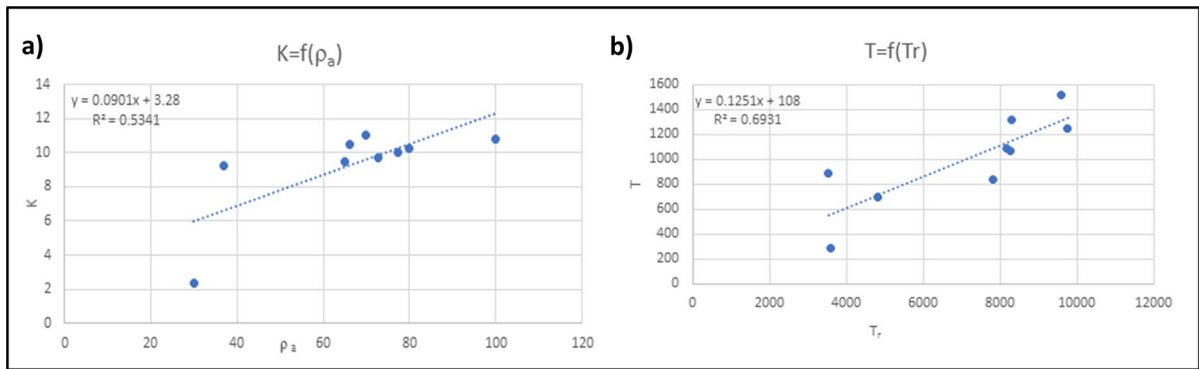


Fig. 5 Relation between transverse resistance, hydraulic conductivity and transmissivity

4 Results

4.1 Geoelectrical interpretation and lithological calibration

First, all 40 apparent resistivity curves were qualitatively interpreted through visual examination to determine the geological model within the surveyed area. Subsequently, a quantitative analysis was performed using IP2WIN software to determine the number of layers and their true resistivity. However, resistivity is sensitive to variations in soil composition and condition. Indeed, different lithologies can produce the same geoelectrical response due to their permeability, pore water content and quality, and clay fraction content. This renders electrical data interpretation quite ambiguous and complex. To overcome this limitation, a detailed understanding of the area's geology is required. In fact, prior in-depth knowledge of the different existing lithology in the area can constrain the inversion model and provide more accurate interpretation.

The interpretation of the various soundings carried out during this work was based on lithological data from eight boreholes distributed throughout the study area. Geoelectrical soundings performed near these boreholes were compared and calibrated against the lithological logs (Fig. 6). This allowed the interpretation of soundings where lithological data was not available and resulted in a local resistivity scale for the region presented in Table 2. However, this resistivity scale is only valid and relevant for the study area since each lithology has

different resistivity values depending on its composition and subsurface conditions.

Based on the results, a NNW-SSE geoelectrical section was constructed to illustrate the lateral and vertical variation of resistivity in the prospected area over a 130 m depth (Fig. 7). This profile reveals a high resistivity interface corresponding to sands and gravels overlying a conductive layer that probably corresponds to the Astian sandstone. At the NNW end, a decrease in resistivity could be caused by seawater infiltration, while the low resistivity at the SSE end may be due to upwelling of salt-rich Astian water through the permeable gravel layer.

4.2 Hydraulic conductivity and transmissivity

The hydraulic parameters were calculated to assess groundwater storage in the study area. First, transmissivity (T) and hydraulic conductivity (K) were measured for the selected VES locations adjacent to the well sites listed in Table 1. Then, a relationship between calculated hydraulic conductivity (K) and aquifer resistivity (ρ_a), and another empirical relationship between measured transmissivity (T) and transverse resistance (T_r) were used to calculate hydraulic conductivity (K_{est}) and transmissivity (T_{est}) for all VES locations. Aquifer parameters obtained by pumping test (K_w and T_w) and calculated aquifer parameters (K_{est} and T_{est}) indicate a good correlation for all selected stations (Table 3). The maps of estimated parameters (Fig. 8a, b) clearly delineates 3 aquifer potential zones. The first zone is marked by $K_{est} > 10.5$ m/day and $T_{est} > 1750$ m²/day, the second zone by $K_{est} < 7.5$ m/day and $T_{est} < 1500$ m²/day, and

Table 1 Estimated values of aquifer resistivity, water resistivity, aquifer thickness, longitudinal conductance, transverse resistance, electrical Conductivity, formation factor, porosity, transmissivity and hydraulic conductivity at the selected 9 VES near the boreholes with available pumping tests

VES no.	H (m)	ρ_0 (Ωm)	T_r (Ωm^2)	S (Ω^{-1})	EC ($\mu\text{S}/\text{cm}$)	ρ_w (Ωm)	$F_a = \rho_0/\rho_w$	$1/F_a$	α	m	Porosity Φ	K (m/day)	T (m^2/day)
S12	144.7	66.2	9579.14	17.76916	1228	8.14	8.13	0.123	1	1.95	0.25813	10.511	1520.965
S14	119	69.8	8306.2	28.798	2420	4.13	16.89	0.059	1	1.97	0.26170	11.060	1316.149
S17	122	80	9760	29.89	2450	4.08	19.60	0.051	1	1.94	0.25634	10.244	1249.727
S21	74.2	65	4823	17.437	2350	4.26	15.28	0.065	1	1.91	0.25091	9.469	702.573
S22	78.1	100	7810	16.1667	2070	4.83	20.70	0.048	1	1.96	0.25992	10.783	842.174
S28	107	77.2	8260.4	19.2493	1799	5.56	13.89	0.072	1	1.93	0.25453	9.981	1067.943
S30	95.8	36.83	3528.314	39.9486	4170	2.40	15.36	0.065	1	1.9	0.24909	9.219	883.212
S27	120	30	3600	12.696	1058	9.45	3.17	0.315	1	1.49	0.16993	2.395	287.419
S37	112	72.8	8153.6	29.904	2670	3.75	19.44	0.051	1	1.92	0.25273	9.722	1088.914

the third between these two zones was revealed with K_{est} varying from 7.5 to 10.5 m/day and T_{est} from 1500 to 1750 m^2/day .

To validate the estimated parameters, a comparison with the calculated parameters is performed. These parameters are depth of water table, saturated thickness, and transmissivity. The results indicate a good correlation that can be improved with additional well measurements to better interpret the geoelectrical data.

4.3 Transverse resistance and longitudinal conductance

Dar-Zarrouk parameters known as longitudinal conductance (S) and transverse resistance (T_r) were estimated using various combinations of resistivity and layer thickness obtained from the inverted VES data. The estimated values of T_r and S for the nine VESs are given in Table 1. T_r values increase with grain size and fresh water, while S values decrease with grain size and fresh water (Hasan et al. 2020a; Iduma et al. 2016). The freshwater aquifer zone was delineated by $T_r > 8000$ (Ωm^2) and $S < 2$ (mho) with sand and gravely sand. The brackish aquifer with clayey sand formation was highlighted by $5000 \Omega\text{m}^2 < T_r < 8000 \Omega\text{m}^2$ and $2 \text{ mho} < S < 2.4 \text{ mho}$. The saline water with clay was evaluated by $T_r < 5000$ (Ωm^2) and $S > 2.4 \text{ mho}$. The T_r and S maps illustrate the distribution of saline, brackish, and fresh aquifer zones throughout the region (Fig. 9a, b). The saline, brackish, and fresh aquifer zones differentiated by T_r and S show a strong correlation with each other.

4.4 Longitudinal and transverse resistivity

For anisotropic aquifers, the prevailing current flow is vertical if the aquifer is clayey and overlying a conductive layer (Niwas and Singhal 1981). This may occur because, if the aquifer resistivity is significantly higher than the underneath conductive layer, the electric current flow will tend to bypass the resistant layer and follow the shortest path to the undermost conductive layer (Akhter and Hasan 2016; Kenneth and Ebifuro 2012). Therefore, the flow lines of the current will be primarily perpendicular to the layer. However, if the aquifer is anisotropic with clay dispersed in sand, the horizontal component of the current may

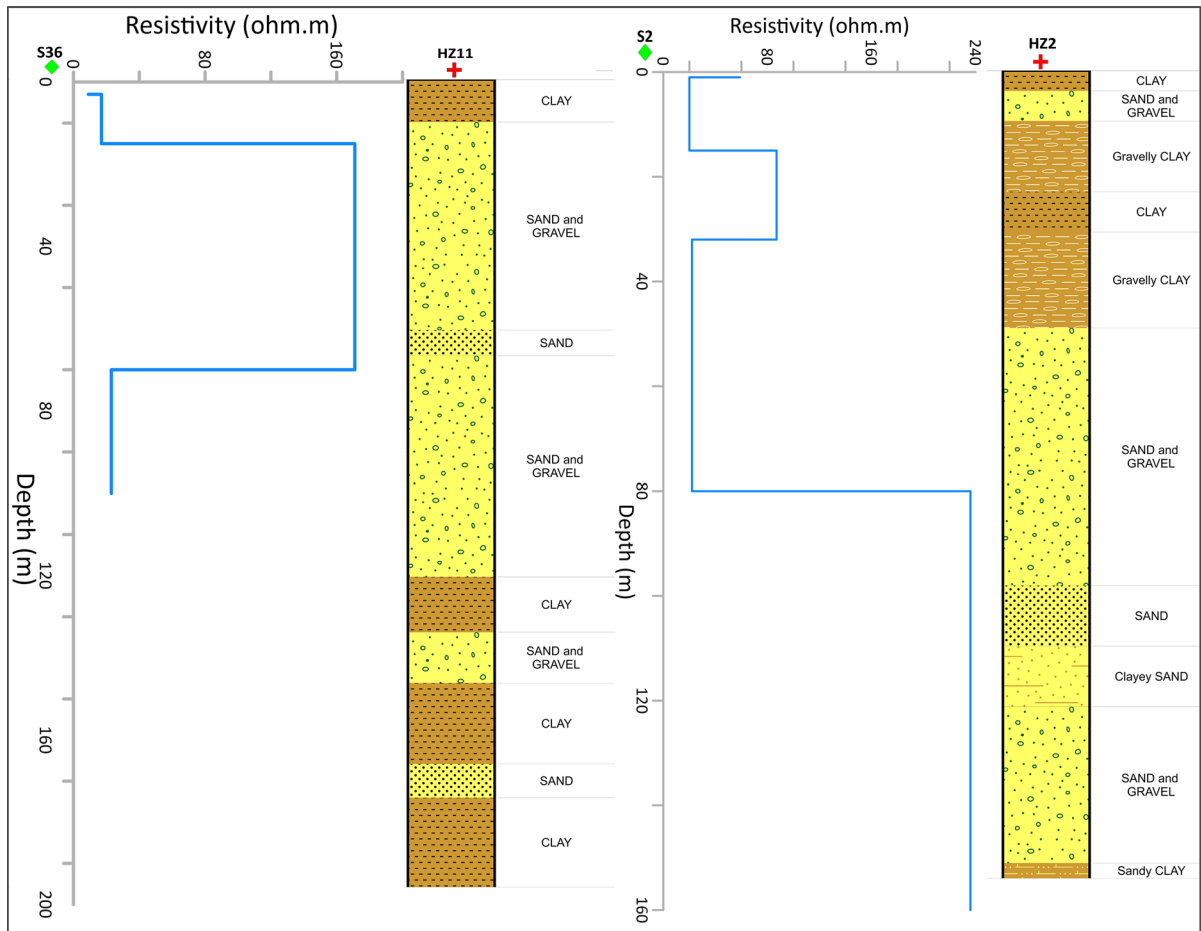


Fig. 6 Comparison between geoelectrical data and lithological logs

Table 2 Local resistivity scale derived from VES interpretation

Formation resistivity (Ωm)	Lithology
< 15 (above water table)	Clay
> 15 (above water table)	Dray strata
< 15 (below water table)	Clay with saline water
$15 < \rho < 30$ (below water table)	Mixture of sand and clay with brackish water
$30 < \rho < 50$ (below water table)	Sand with fresh water
> 50 (below water table)	Mixture of sand and gravel with fresh water

be significant due to the conductive clay (Sinha et al. 2009).

The ρ_1 was also used to distinguish between saline, brackish, and fresh water zones. The 10 m contour interval map is plotted for all values, as shown in Fig. 10. These represent very simple,

visible, and very different intervals in three different regions for the saline, brackish, and freshwater aquifers based on the widths obtained. For the saline water aquifer, the ρ_1 is $< 30 \Omega\text{m}$; from 30 to $60 \Omega\text{m}$ for the brackish water aquifer; and $\rho_1 > 60 \Omega\text{m}$ for the freshwater aquifer. The values of ρ_t were also

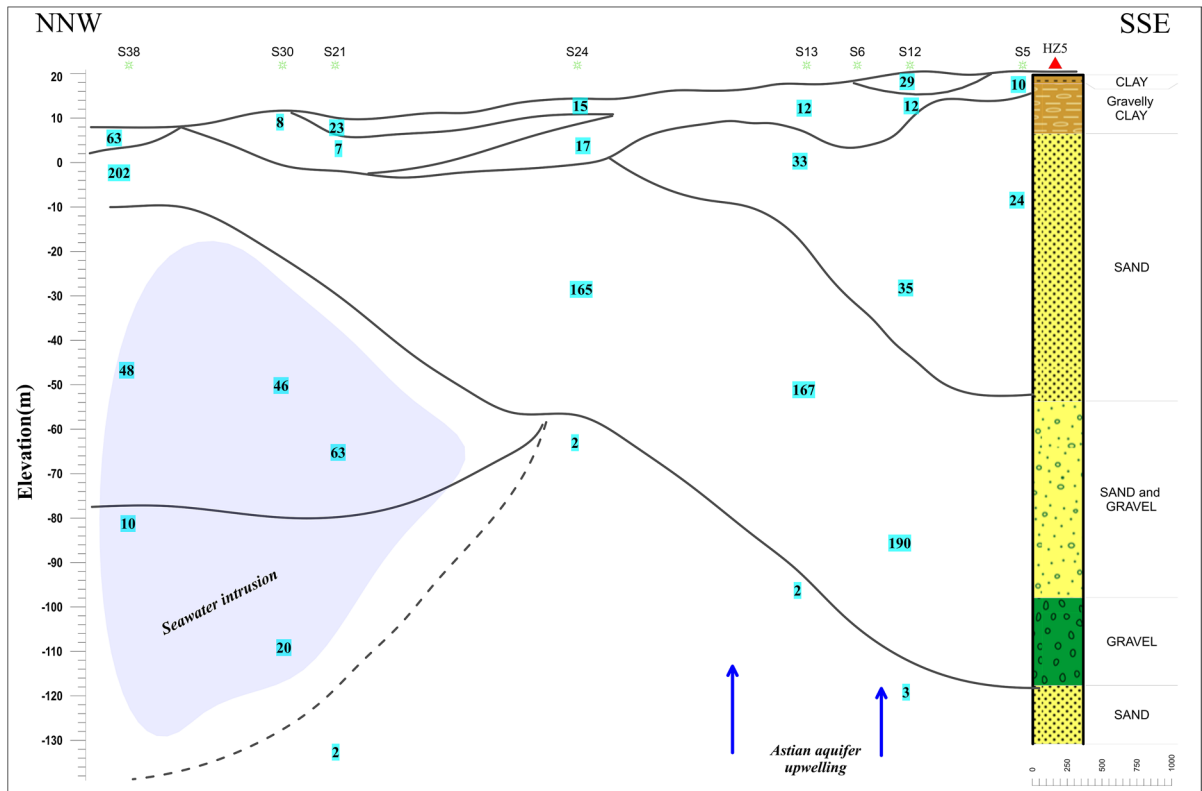


Fig. 7 Geoelectrical cross section oriented NNW-SSE with a schematic proposition of salinity causes in the study area

plotted as shown in Fig. 10b. The value less than 90 Ωm indicates the presence of salt water, values between 90 and 110 indicate the presence of brackish water while values greater than 110 indicate the presence of fresh water. On the other hand, Keller and Frischknecht (1966) report that the anisotropic

coefficient (λ) increases with compaction and rock hardness. Unlike the other parameters, including S , T_r , ρ_t , and ρ_f , saline, brackish, and freshwater properties could not be distinguished from the anisotropic coefficient contour map (Fig. 10c). The reason for the unclear properties could be the irregular

Table 3 Comparison between estimated and pumping test parameters for the selected nine VES and boreholes location

VES no.	CV water depth (m)			CV aquifer thickness (m)			CV transmissivity (m^2/day)		
	Measured	Predicted	Error	Measured	Predicted	Error	Measured	Predicted	Error
S12	32.00	65.70	33.70	150.00	111.00	- 39.00	1100.00	1006.44	- 93.56
S14	33.00	14.60	- 18.40	41.82	55.40	13.58	1300.00	502.31	- 797.69
S17	48.00	36.10	- 11.90	154.00	122.00	- 32.00	1000.00	1106.17	106.17
S21	17.00	11.00	- 6.00	104.54	74.20	- 30.34	1050.00	672.77	- 377.23
S22	31.00	10.00	- 21.00	96.68	78.10	- 18.58	980.00	708.13	- 271.87
S28	12.00	9.06	- 2.94	80.19	107.00	26.81	750.00	970.17	220.17
S30	15.00	4.98	- 10.02	99.10	95.80	- 3.30	930.00	868.62	- 61.38
S27	12.00	19.90	7.90	86.23	120.00	33.77	750.00	1088.04	338.04
S37	44.00	28.30	- 15.70	142.24	112.00	- 30.24	1350.00	1015.50	- 334.50

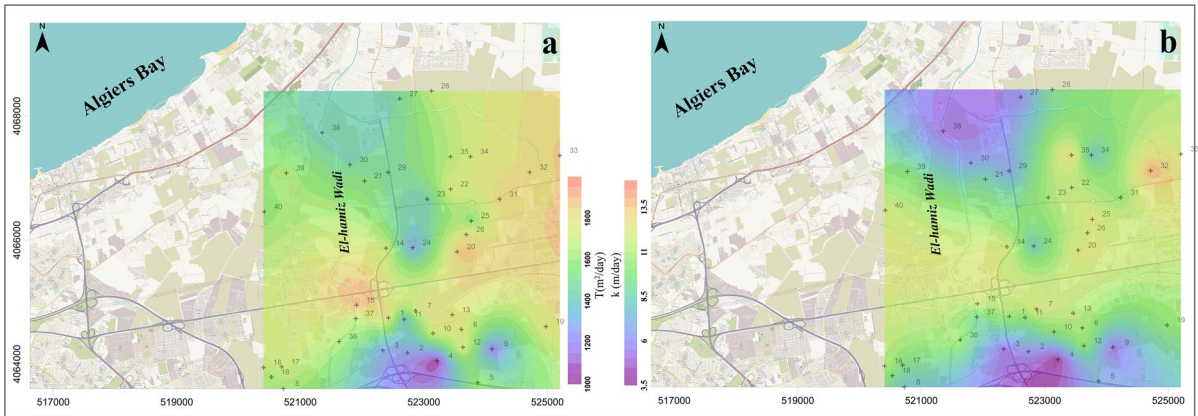


Fig. 8 Hydraulic parameters distribution over the study area: **a** transmissivity map and **b** hydraulic conductivity map

distribution of clay and sand. However, according to Flathe (1955a, b), anisotropy results from alternating layers of clay and fine sand, and Frohlich (1974) indicates that anisotropy is the impact of intercalation of different grains in equivalent layers. This is consistent with the geology of the study area, marked by heterogeneous formations.

4.5 Physico-chemical analysis

Based on the results of this study, groundwater samples were collected from the study area for physico-chemical analysis to enhance the results obtained by the geophysical method. The analytical results of physicochemical parameters were obtained in the form of statistical parameters such as minimum,

maximum, mean, median and standard deviation as shown in Table 4. The results of the physicochemical analysis suggest that the groundwater samples that do not exceed the WHO suggested limits for drinking water have good water quality (freshwater). Groundwater samples that exceed the suggested limits for most physicochemical parameters such as EC, Na, Mg, Cl, SO₄ and HCO₃ indicate poor water quality (saline water). Groundwater samples that exceed the suggested limit for some of the physicochemical parameters such as EC or Na⁺ show average water quality (brackish water). The results of the physicochemical analyses for drinking water quality show a good correlation with the saline, brackish and fresh aquifers revealed by the geo-electric method.

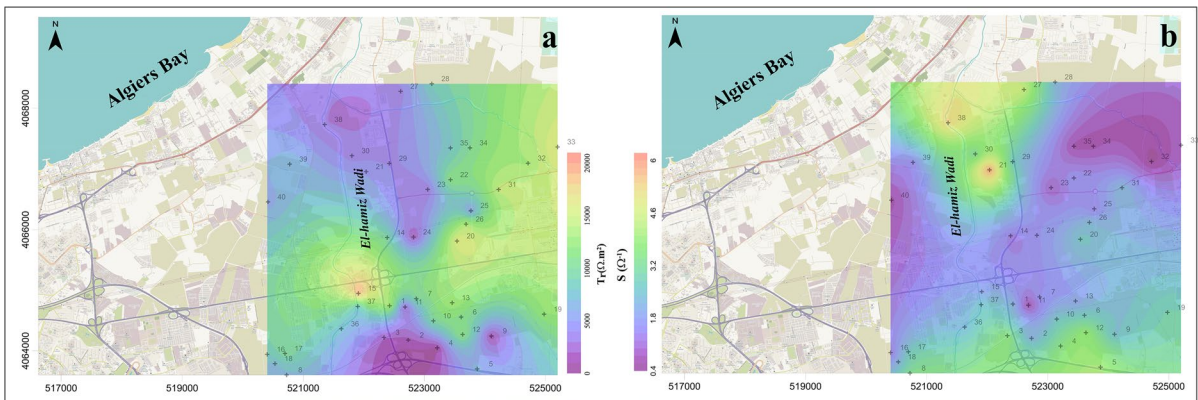


Fig. 9 **a** Transverse resistance map and **b** longitudinal conductance map

5 Discussion

Access to groundwater has become a major concern in many countries. Understanding the different factors and characteristics of these aquifers is crucial for their sustainable development to ensure a regular access to fresh water. The focus of this study is to address the estimation of hydraulic parameters (**K** and **T**) necessary for the implementation of new water wells. The second is the evaluation of water quality in the study area.

The hydraulic parameters estimated from the geoelectrical data showed a good correlation with the values measured by pumping tests. The estimated values range from 1000 to 2000 (m^2/day) and from 3.5 to 14.5 (m/day) for **T** and **K** respectively. These values are close to those determined by an expensive and slow pumping test. This indicates that the technique used could be extended to other regions to minimize the cost and duration of

hydrogeological investigations (Benabdelouahab et al. 2019; Hermans 2014). Indeed, geoelectrical techniques are widely applied to characterize the geometry, structure, quality and hydraulic properties of aquifers. A major drawback of vertical electrical soundings, however, is their ability to measure resistivity in only one dimension and not detect horizontal (or lateral) changes in subsurface resistivity. These changes influence the apparent resistivity and can be misinterpreted as resistivity variations at depth. Electrical Resistivity Imaging can provide a supplementary alternative to overcome these limitations. In fact, this technique can map the vertical and horizontal variation of resistivity along a profile, thereby significantly reducing interpretation errors. Aside from this, a proper interpretation of any geoelectrical result is necessary based on the problem at hand and the data available. Furthermore, a reliability test is essential, particularly when these approaches are used to estimate the hydraulic properties of an aquifer.

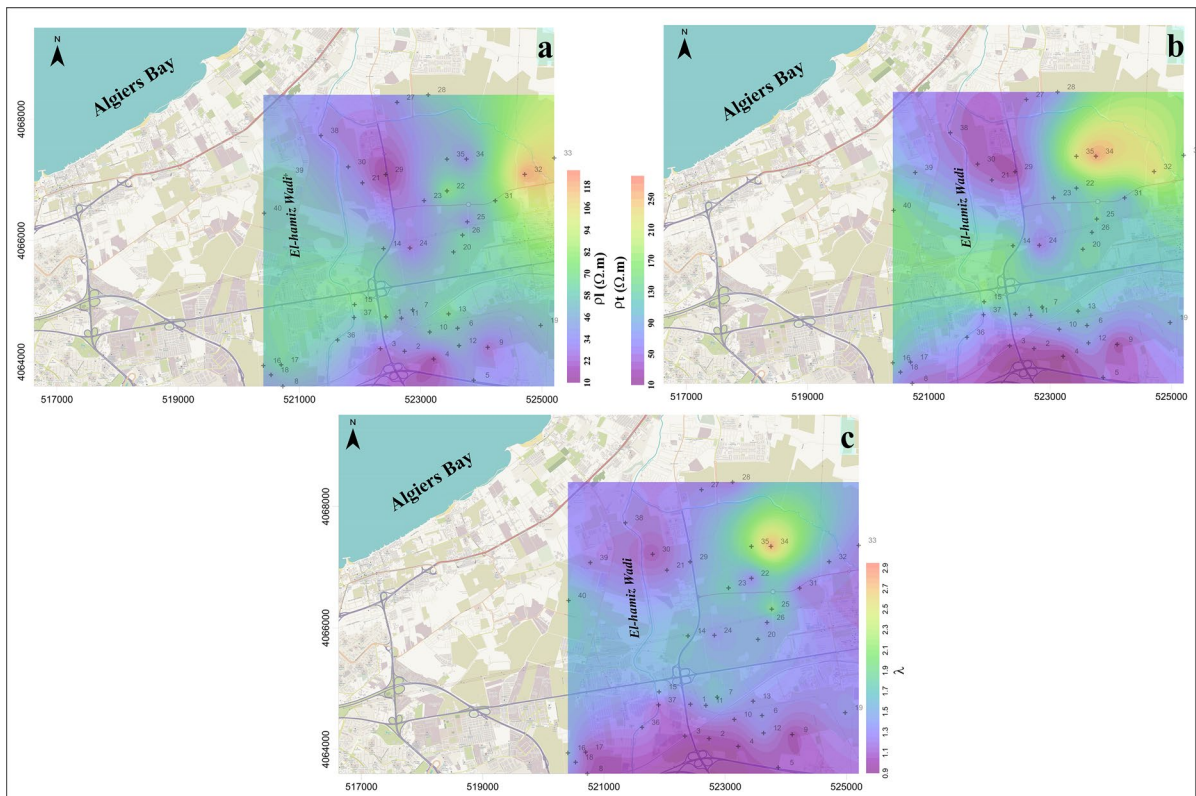


Fig. 10 Dar-Zarrouk parameters: **a** transverse resistivity map, **b** longitudinal resistivity map, **c** anisotropic coefficient map

Theoretically, when the subsurface presents uniform formations, changes in resistivity within the aquifer layer are often explained by a variation of electrolyte concentration (Cl^-). Therefore, assessment of groundwater quality using geoelectrical data is relatively simple if conductivity measurements of the groundwater samples are concurrently conducted. Ideally, geoelectrical techniques are most appropriate to such investigations when combined with several carefully located wells to correlate true resistivity and Cl content (Flathe 1955b). However, challenges appear when conducting resistivity measurements over heterogeneous subsurface. This is the case of our study area where clay layers of varying thicknesses are deposited in channels and pockets due to morphoclimatic conditions. In addition, these clays present frequent facies change as they occur as rich clay layers, more or less sandy clay layer and sometimes as series of alternating layers of fine sand and clay. These clay occurrences present a wide range of resistivity that increases with depth. For any hydrogeological studies, it is important to distinguish between clay layers and saltwater-bearing reservoirs. In this matter, Dar-Zarrouk parameters as a combination of thickness and resistivity have emerged as a useful tool to estimate aquifers parameters and its protective capacity (Henriet 1976).

Five major parameters were calculated and mapped in this study including: Transverse resistance, longitudinal conductance, transverse resistivity, longitudinal resistivity and anisotropic coefficient. All these parameters were initially used to assess the groundwater quality within the study area and revealed three

zones. The first zone is towards the north and is identified as an area contaminated by seawater probably caused by excessive groundwater intake combined with insufficient rainfall to replenish the aquifer. The second area is defined as a freshwater zone and covers the central part of the survey area. This area is also characterized by high transmissivity and hydraulic conductivity which accounts for the number of wells located in this area. Based on the maps, a privileged corridor of saline water infiltration is noticeable. This path follows El Hamiz Wadi and it may be due to the presence of permeable formations of increased transmissivity that favor the rapid advance of the salt water/fresh water interface. This has been evidenced by electrical conductivity measurements as shown in Fig. 11. However, the southern part also presents features of degraded groundwater that cannot be explained by a marine intrusion. As mentioned in the presentation of the study area, two aquifers exist in the area that are in direct contact or separated by permeable gravel deposits. This development provides an outflow from the deep aquifer characterized by a high salt content. Moreover, this interaction is accelerated due to the overexploitation of the quaternary aquifer. Indeed, due to the significant decline in the piezometric level, farmers increase the well depth and lower their pumps, which promotes the upwelling of Astian water. Nevertheless, this interaction remains theoretical and more in-depth studies should be conducted to determine the origin of the groundwater degradation in this area.

Groundwater quality is usually determined by hydrochemical analysis of water samples collected

Table 4 Statistical analysis of hydro-chemical analysis results

Variables	Observations	Min	Max	Mean	Standard deviation	Permissible range (WHO)
Ca^{2+} (mg/l)	14	30	304	129	80.44	100
Mg^{2+}	14	17	240	66	56.75	50
Na^+	14	32	320	141	77.72	200
K^+	14	0	20	5	6.1	55
Cl^-	14	77	1600	307	269.77	250
SO_4^{2-}	14	30	319	198	89.35	200
NO_3^-	14	107	641	42	37.27	45
HCO_3^-	14	0	120	274	131.63	600
pH	22	7.1	8.3	7.8	0.45	6.5–8.5
EC ($\mu\text{S}/\text{cm}$)	22	502	6000	2199	1192.59	1500

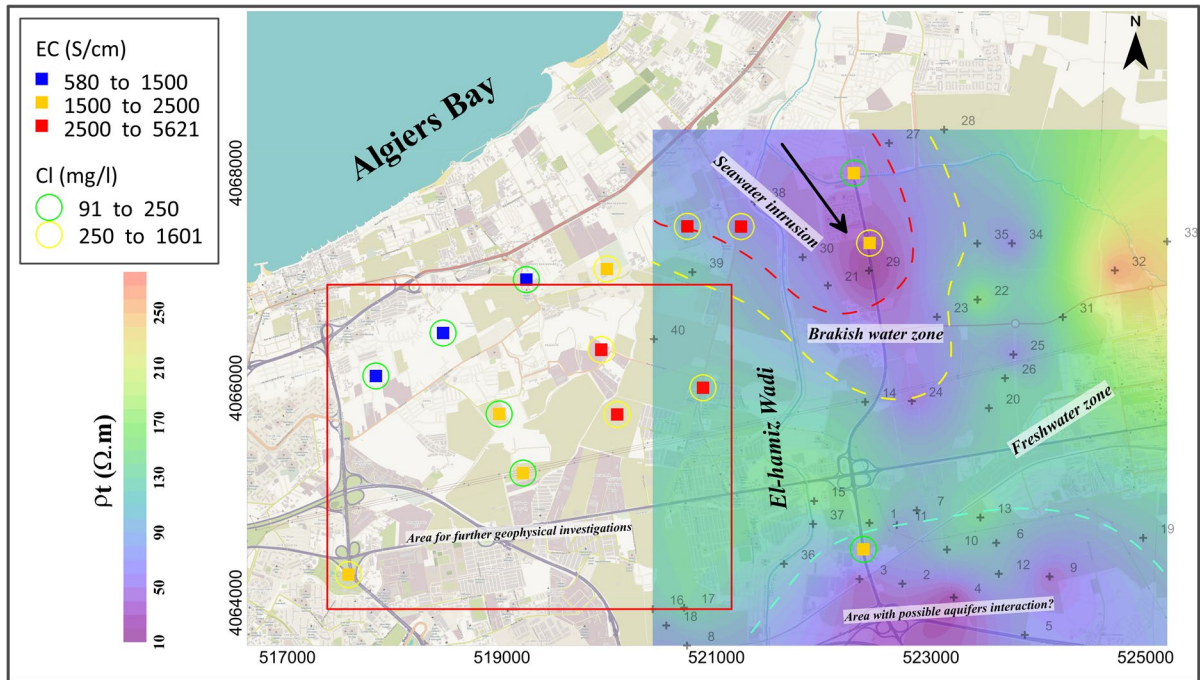


Fig. 11 Overlay of transverse resistivity map with EC and Cl content measurements with a proposed delimitation of various zones identified

from wells. This technique provides accurate results but is slow and time consuming. For this study, water samples were collected from available wells in the study area to assess the water quality and compare the results with geophysical data. As shown in the Fig. 11, the results are consistent with those obtained by geoelectrical methods.

6 Conclusion

Given the rapid increase in water demand, understanding and assessment of groundwater aquifers is essential for their sustainable management. In the present study, a multidisciplinary approach was adopted to determine the aquifer parameters and assess its groundwater quality. The results indicate that geoelectrical studies can accurately identify the lithology of a given area and estimate the hydraulic parameters usually determined using expensive and time-consuming techniques. These results will help to identify the most appropriate areas for the implantation of new water wells or the extension of existing well fields. Furthermore, the spatial distribution of the

Dar-Zarrouk parameters revealed significant seawater contamination towards the north of the study area and a degradation of groundwater quality towards the south possibly related to an interaction between the deep Astian and the shallow Quaternary aquifer. Based on the geophysical results and hydrochemical analysis, two main issues require further investigation, if possible through a combination of geophysical and hydrogeological methods. First, the marine intrusion phenomenon must be carefully assessed over the entire study area, especially toward the west where geophysical data are lacking but hydrochemical analyses indicate high electrical conductivity and Cl content. The infiltration pathway needs to be accurately mapped to restrict pumping rates in this area. Second, the water quality degradation towards the south requires thorough investigation and evaluation. Indeed, many authors and reports refer to a possible interaction between the two aquifers but this phenomenon has not been quantitatively evaluated. In addition, with the rapid population growth and the increase in periods of drought, the groundwater resource of this area is undoubtedly facing a serious risk, increased by its proximity to the coastline. It is

therefore essential that the authorities develop appropriate management strategies to protect this resource and ensure its sustainability. Geophysical methods have proven to be reliable in supporting the above process and the results of this and future studies may contribute to reducing the data gap between the available data and the information required for groundwater monitoring.

Acknowledgements We would like to thank the anonymous reviewer for their valuable comments that helped enhance the quality of our paper. Special thanks to Andrew Binley, Ibrahim Abbad, Mohamed Hamoudi and Sawsen Belhadj Aissa for the insightful conversations we had regarding the paper.

Declarations

Competing interests The authors declare that they have no competing interests.

Open Access This article is licensed under a Creative Commons Attribution 4.0 International License, which permits use, sharing, adaptation, distribution and reproduction in any medium or format, as long as you give appropriate credit to the original author(s) and the source, provide a link to the Creative Commons licence, and indicate if changes were made. The images or other third party material in this article are included in the article's Creative Commons licence, unless indicated otherwise in a credit line to the material. If material is not included in the article's Creative Commons licence and your intended use is not permitted by statutory regulation or exceeds the permitted use, you will need to obtain permission directly from the copyright holder. To view a copy of this licence, visit <http://creativecommons.org/licenses/by/4.0/>.

References

- Abdelrahman E-SM, Essa KS, Abo-Ezz ER, Sultan M, Sauck WA, Ghariieb AG (2008) New least-squares algorithm for model parameters estimation using self-potential anomalies. *Comput Geosci* 34(11):1569–1576
- Adepelumi AA, Yi MJ, Kim JH, Ako BD, Son JS (2006) Integration of surface geophysical methods for fracture detection in crystalline bedrocks of southwestern Nigeria. *Hydrogeol J* 14(7):1284–1306. <https://doi.org/10.1007/S10040-006-0051-2>
- Akhter G, Hasan M (2016) Determination of aquifer parameters using geoelectrical sounding and pumping test data in Khanewal District. *Pak Open Geosci* 8(1):630–638. <https://doi.org/10.1515/GEO-2016-0071>
- Akhter G, Ge Y, Hasan M, Shang Y (2022) Estimation of hydrogeological parameters by using pumping, laboratory data, surface resistivity and Thiesse technique in Lower Bari Doab (Indus Basin). *Pak Appl Sci (switzerland)* 12(6):1–19. <https://doi.org/10.3390/app12063055>
- ANRH (1977) SCHEMA GENERAL DE L'AMENAGEMENT HYDRAULIQUE DE LA MITIDJA VOLUME IV: ETUDES GEOLOGIQUES ET HYDROGEOLOGIQUES
- ANRH (2012) Evolution of the piezometric Mitidja aquifer Note. ANRH Report. p. 46
- Aymé A (1952) Le Quaternaire littoral des environs d'Alger. Actes Du Congrès Panafricain de Préhistoire, Ite Session, Alger, pp 242–246
- Bahr, K. (2007). Anisotropy, electrical. *Encyclopedia of Geomagnetism and Paleomagnetism*, pp 20–21. https://doi.org/10.1007/978-1-4020-4423-6_7
- Bateni SM, Mortazavi-Naeini M, Ataie-Ashtiani B, Jeng DS, Khanbilvardi R (2015) Evaluation of methods for estimating aquifer hydraulic parameters. *Appl Soft Comput* 28:541–549. <https://doi.org/10.1016/J.ASOC.2014.12.022>
- Bear J, Braester C (1972) On the flow of two immiscible fluids in fractured porous media. In: *Developments in soil science*, vol 2, pp 177–202. Elsevier
- Belaidi M, Salhi M (2010) Note sur la piezometrie de la nappe de la Mitidja (campagne2010)
- Benabdellouahab S, Salhi A, Himi M, StitouElMessari JE, CasasPonsati A (2019) Geoelectrical investigations for aquifer characterization and geoenvironmental assessment in northern Morocco. *Environ Earth Sci*. <https://doi.org/10.1007/s12665-019-8221-4>
- Betrouni M (1983) Le pléistocène supérieur du littoral ouest algérois
- Binley A (2015) Tools and techniques: electrical methods. *Treat Geophys* 11:233–259. <https://doi.org/10.1016/B978-0-444-53802-4.00192-5>
- Cross K, Laban P, Paden M, Smith M (2016) Spring: managing groundwater sustainably
- de Lima OAL, Sharma MM (1990) A grain conductivity approach to shaly sandstones. *Geophysics* 55(10):1347–1356
- Djediati Y (1996) Etude géologique et géotechnique de la mitidja nord orientale. University of sciences and technology Houari Boumediene
- Djediati Y (2013) Le domaine margino-littoral algérois organisation et évolution néogène et quaternaire, implications géotechniques et prospects pour une occupation rationnelle des espaces
- Ebong ED, Akpan AE, Onwuegbuche AA (2014) Estimation of geohydraulic parameters from fractured shales and sandstone aquifers of Abi (Nigeria) using electrical resistivity and hydrogeologic measurements. *J Afr Earth Sci* 96:99–109. <https://doi.org/10.1016/J.JAFREARSCL.2014.03.026>
- El Osta M, Masoud M, Badran O (2021) Aquifer hydraulic parameters estimation based on hydrogeophysical methods in West Nile Delta, Egypt. *Environ Earth Sci*. <https://doi.org/10.1007/S12665-021-09617-3>
- Flathe H (1955a) A practical method of calculating geoelectrical model graphs for horizontally stratified media. *Geophys Prospect* 3(3):268–294
- Flathe H (1955b) Possibilities and limitations in applying geoelectrical methods to hydrogeological problems in the coastal areas of North West Germany. *Geophys Prospect* 3(2):95–109. <https://doi.org/10.1111/j.1365-2478.1955.tb01363.x>

- Frohlich RK (1974) Combined geoelectrical and drill-hole investigations for detecting fresh-water aquifers in north-western Missouri. *Geophysics* 39(3):340–352
- Ginzburg A (1974) Resistivity surveying. *Geophys Surv* 1(3):325–355
- Glangeaud L (1952) Tectonophysique comparee des chaines telliennes et rifaines. *Bulletin De La Société Géologique De France* 6(7–9):619–639
- Hadjoudj O, Bensemmane R, Saoud Z, Reggabi M (2014) Pollution des eaux souterraines de la mitidja par les nitrates: État des lieux et mesures correctives. *Eur J Water Qual* 45:57–68. <https://doi.org/10.1051/wqual/20140010>
- Haldar SK (2013) Exploration geophysics. *Miner Explor*. <https://doi.org/10.1016/B978-0-12-416005-7.00005-2>
- Hasan M, Shang Y, Akhter G, Khan M (2017) Geophysical investigation of fresh-saline water interface: a case study from south Punjab. *Pak Groundw* 55(6):841–856
- Hasan M, Shang Y, Akhter G, Jin W (2018) Geophysical assessment of groundwater potential: a case study from Mian Channu Area. *Pak Groundw* 56(5):783–796. <https://doi.org/10.1111/gwat.12617>
- Hasan M, Shang Y, Metwaly M, Jin W, Khan M, Gao Q (2020a) Assessment of groundwater resources in coastal areas of Pakistan for sustainable water quality management using joint geophysical and geochemical approach: a case study. *Sustainability (switzerland)* 12(22):1–23. <https://doi.org/10.3390/su12229730>
- Hasan M, Shang Y, Metwaly M, Jin W, Khan M, Gao Q (2020b) Assessment of groundwater resources in coastal areas of Pakistan for sustainable water quality management using joint geophysical and geochemical approach: a case study. *Sustainability* 12:9730. <https://doi.org/10.3390/su12229730>
- Hasan M, Shang Y, Jin W, Akhter G (2021) Estimation of hydraulic parameters in a hard rock aquifer using integrated surface geoelectrical method and pumping test data in southeast Guangdong, China. *Geosci J* 25(2):223–242. <https://doi.org/10.1007/S12303-020-0018-7>
- Henriet JP (1976) Direct applications of the Dar Zarrouk parameters in ground water surveys. *Geophys Prospect* 24(2):344–353
- Hermans TJ (2014) Integration of near-surface geophysical, geological and hydrogeological data with multiple-point geostatistics in alluvial aquifers. 297. <http://orbi.ulg.ac.be/handle/2268/163547>
- Iduma REO, Abam TKS, Uko ED, Iduma REO, Abam TKS, Uko ED (2016) Dar Zarrouk parameter as a tool for evaluation of well locations in Afikpo and Ohaozara, Southeastern Nigeria. *J Water Resour Prot* 8(4):505–521. <https://doi.org/10.4236/JWARP.2016.84043>
- Islam SMF, Karim Z (2019) World's demand for food and water: the consequences of climate change. *Desalin Chall Oppor* 57–84
- Jackson PD, Smith DT, Stanford PN (1978) Resistivity-porosity-particle shape relationships for marine sands. *Geophysics* 43(6):1250–1268
- Keller GV, Frischknecht FC (1966) Electrical methods in geophysical prospecting.
- Kenneth SO, Ebifuro O (2012) Geoelectric sounding for the determination of aquifer transmissivity in parts of Bayelsa State, South Nigeria. *J Water Resour Prot* 2012(06):346–353. <https://doi.org/10.4236/JWARP.2012.46039>
- Kneisel C, Hauck C (2008) Electrical methods. *Appl Geophys Periglac Environ*. <https://doi.org/10.1017/CBO9780511535628.002>
- Konikow LF, Kendy E (2005) Groundwater depletion: a global problem. *Hydrogeol J* 13(1):317–320. <https://doi.org/10.1007/S10040-004-0411-8>
- Kosinski WK, Kelly WE (1981) Geoelectric soundings for predicting aquifer properties. *Groundwater* 19(2):163–171. <https://doi.org/10.1111/J.1745-6584.1981.TB03455.X>
- Maillet R (1947) The fundamental equations of electrical prospecting. *Geophysics* 12(4):529–556
- Mantovani M (2016) Near-surface modeling: a multiphysics approach. *Lead Edge*. <https://doi.org/10.1190/TLE35110968.1>
- Margat J, van der Gun J (2013) Groundwater around the world : a geographic synopsis. *Groundw around World*. <https://doi.org/10.1201/B13977>
- Massoud U, Soliman M, Taha A, Khozaym A, Salah H (2015) 1D and 3D inversion of VES data to outline a fresh water zone floating over saline water body at the northwestern coast of Egypt. *NRIAG J Astron Geophys* 4(2):283–292. <https://doi.org/10.1016/J.NRJAG.2015.11.001>
- Mepaiyeda S, Madi K, Gwavava O, Baiyegunhi C, Sigabi L (2019) Contaminant delineation of a landfill site using electrical resistivity and induced polarization methods in Alice, Eastern Cape, South Africa. *Int J Geophys*. <https://doi.org/10.1155/2019/5057832>
- Mlangi TM, Mulibo GD, Mlangi TM, Mulibo GD (2018) Delineation of shallow stratigraphy and aquifer formation at Kahe Basin, Tanzania: implication for potential aquiferous formation. *J Geosci Environ Prot* 6(1):78–98. <https://doi.org/10.4236/GEP.2018.61006>
- Moore WS, Joye SB (2021) Saltwater intrusion and submarine groundwater discharge: acceleration of biogeochemical reactions in changing coastal aquifers. *Front Earth Sci*. <https://doi.org/10.3389/FEART.2021.600710>
- Mundry E, Dennert U (1980) Das Umkehrproblem in der Geoelektrik. *Geol Jb E* 19:19–38
- Narayan S, Dusseault MB, Nobes DC (1994) Inversion techniques applied to resistivity inverse problems. *Inverse Prob* 10(3):669–686. <https://doi.org/10.1088/0266-5611/10/3/011>
- Niwas S, Singhal DC (1981) Estimation of aquifer transmissivity from Dar-Zarrouk parameters in porous media. *J Hydrol* 50(C):393–399. [https://doi.org/10.1016/0022-1694\(81\)90082-2](https://doi.org/10.1016/0022-1694(81)90082-2)
- Park SG, Shin SW, Lee DK, Kim CR, Son JS (2016) Relationship between electrical resistivity and physical properties of rocks. In: 22nd European meeting of environmental and engineering geophysics, near surface geoscience 2016. <https://doi.org/10.3997/2214-4609.201602101>
- Pozdnyakova L, Pozdnyakov A, Zhang R (2001) Application of geophysical methods to evaluate hydrology and soil properties in urban areas. *Urban Water* 3(3):205–216. [https://doi.org/10.1016/S1462-0758\(01\)00042-5](https://doi.org/10.1016/S1462-0758(01)00042-5)
- Samouëlian A, Cousin I, Tabbagh A, Bruand A, Richard G (2005) Electrical resistivity survey in soil science: a review. *Soil till Res* 83(2):173–193. <https://doi.org/10.1016/J.STILL.2004.10.004>

- Singh UK, Das RK, Hodlur GK (2003) Significance of Dar-Zarrouk parameters in the exploration of quality affected coastal aquifer systems. *Environ Geol* 45(5):696–702. <https://doi.org/10.1007/S00254-003-0925-8>
- Singhal BBS, Gupta RP (1999) Applied hydrogeology of fractured rocks. *Appl Hydrogeol Fract Rocks*. <https://doi.org/10.1007/978-94-015-9208-6>
- Sinha R, Israil M, Singhal DC (2009) A hydrogeophysical model of the relationship between geoelectric and hydraulic parameters of anisotropic aquifers. *Hydrogeol J* 17(3):495
- Tijani MN, Obini N, Inim IJ (2021) Estimation of aquifer hydraulic parameters and protective capacity in basement aquifer of south-western Nigeria using geophysical techniques. *Environ Earth Sci*. <https://doi.org/10.1007/S12665-021-09759-4>
- Utom AU, Odoh BI, Okoro AU (2012) Estimation of aquifer transmissivity using Dar Zarrouk parameters derived from surface resistivity measurements: a case history from parts of Enugu Town (Nigeria). *J Water Resour Prot* 04(12):993–1000. <https://doi.org/10.4236/JWARP.2012.412115>
- Waxman MH, Smits LJM (1968) Electrical conductivities in oil-bearing shaly sands. *Soc Pet Eng J* 8(02):107–122
- Worthington PF (1993) The uses and abuses of the Archie equations, 1: the formation factor-porosity relationship. *J Appl Geophys* 30(3):215–228
- Yassini I (1973) Nouvelles données stratigraphiques et microfaunistiques sur la limite Pliocène inférieur-Pliocène moyen (Plaisancien-Astien) dans la région d'Alger. *Rev Micropaléontol* 16(4):229–248
- Zohdy AAR, Eaton GP, Mabey DR (1974) Application of surface geophysics to ground-water investigations

Publisher's Note Springer Nature remains neutral with regard to jurisdictional claims in published maps and institutional affiliations.